Clin Oral Invest (2017) 21:2671–2679
DOI 10.1007/s00784-017-2069-3

ORIGINAL ARTICLE

Comparison of the effects of recombinant human bone morphogenetic protein-2 and -9 on bone formation in rat calvarial critical-size defects

Toshiaki Nakamura[1] · Yoshinori Shirakata[1] · Yukiya Shinohara[1] · Richard J. Miron[2] · Kozue Hasegawa-Nakamura[1] · Masako Fujioka-Kobayashi[3,4] · Kazuyuki Noguchi[1]

Received: 19 October 2016 / Accepted: 31 January 2017 / Published online: 14 February 2017

Abstract

Objectives Among bone morphogenetic protein (BMP) family members, BMP-2 and BMP-9 have demonstrated potent osteoinductive potential. However, in vivo differences in their potential for bone regeneration remain unclear. The present study aimed to compare the effects of recombinant human (rh) BMP-2 and rhBMP-9 on bone formation in rat calvarial critical-size defects (CSD).

Materials and methods Twenty-eight Wistar rats surgically received two calvarial defects bilaterally in each parietal bone. Defects (n = 56) were allocated into four groups: absorbable collagen sponge (ACS) alone, rhBMP-2 with ACS (rhBMP-2/ACS), rhBMP-9/ACS, or sham surgery (control), on the condition that the treatments of rhBMP-2/ACS and rhBMP-9/ACS, or the same treatments were not included in the same animal. Animals were sacrificed at 2 and 8 weeks post-surgery. The calvarial defects were analyzed for bone volume (BV) by micro-computed tomography and for percentages of defect closure (DC/DL), newly formed bone area (NBA/TA), bone marrow area (BMA/NBA), adipose tissue area (ATA/NBA), central bone height (CBH), and marginal bone height (MBH) by histomorphometric analysis.

Results The BV in the rhBMP-2/ACS group (5.44 ± 3.65 mm^3, n = 7) was greater than the other groups at 2 weeks post-surgery, and the rhBMP-2/ACS and rhBMP-9/ACS groups (18.17 ± 2.51 and 16.30 ± 2.46 mm^3, n = 7, respectively) demonstrated significantly greater amounts of BV compared with the control and ACS groups (6.02 ± 2.90 and 9.30 ± 2.75 mm^3, n = 7, respectively) at 8 weeks post-surgery. The rhBMP-2/ACS and rhBMP-9/ACS groups significantly induced new bone formation compared to the control and ACS groups at 8 weeks post-surgery. However, there were no statistically significant differences found between the rhBMP-2/ACS and rhBMP-9/ACS groups in any of the histomorphometric parameters. The ATA/NBA in the rhBMP-2/ACS group (9.24 ± 3.72%, n = 7) was the highest among the treatment groups at 8 weeks post-surgery.

Conclusions Within the limits of this study, it can be concluded that rhBMP-2/ACS induced a slight early increase in new bone formation at 2 weeks and that rhBMP-9/ACS provided comparable new bone formation to rhBMP-2/ACS with less adipose tissues after a healing period of 8 weeks in rat CSD.

Clinical relevance RhBMP-9/ACS treatment provided new bone formation with less adipose tissues compared with rhBMP-2/ACS.

Keywords Growth factor · Bone morphogenetic protein-2 · Bone morphogenetic protein-9 · Collagen · Bone regeneration

Introduction

Several growth and differentiation factors, including insulin-like growth factor 1, platelet-derived growth factor, fibroblast growth factor 2 (FGF-2), platelet-rich plasma protein, and

Toshiaki Nakamura and Yoshinori Shirakata equally contributed to this work.

✉ Kazuyuki Noguchi
kazuperi@dent.kagoshima-u.ac.jp

[1] Department of Periodontology, Kagoshima University Graduate School of Medical and Dental Sciences, 8-35-1 Sakuragaoka, Kagoshima 890-8544, Japan

[2] Department of Periodontology, Nova Southeastern University, Fort Lauderdale, FL, USA

[3] Department of Cranio-Maxillofacial Surgery, Bern University Hospital, Inselspital, Bern, Switzerland

[4] Department of Oral Surgery, Institute of Biomedical Sciences, Tokushima University Graduate School, Tokushima, Japan

bone morphogenetic proteins (BMPs) have been employed to accomplish predictable bone formation in the fields of periodontology and oral maxillofacial surgery [1, 2]. In particular, BMP-2 has been shown to possess excellent osteoinductive activity and has been extensively studied [3–6]. Some reports have demonstrated that the application of recombinant human BMP-2 (rhBMP-2) with an absorbable collagen sponge (ACS) induces new bone formation in mandibular and cleft palate defects, with results comparable to autogenous bone grafts [3, 7]. However, supraphysiological doses of rhBMP-2 (in the milligram range) reportedly required for osteoinductive effects in humans [8] may produce adverse side effects including edema, erythema, and gingival swelling [9, 10]. Furthermore, high dosages of rhBMP-2 may also induce structurally abnormal bone, such as cyst-like bone void filled with fatty marrow [11]. Accordingly, there remains great interest to identify/develop alternative strategies incorporating growth factors at more reasonable physiological dosages to promote effective osteoinduction and ideal bone regeneration.

Comparative studies using adenovirus-transfection experiments to investigate several BMPs found that BMP-9 (also known as growth/differentiation factor-2) has the greatest in vitro and in vivo osteogenic potential compared with all other BMPs, including clinically approved BMP-2 and BMP-7 [12, 13]. BMP-9, which has been shown to play a pivotal role in many physiological processes including neuronal and adipocyte differentiation [14, 15], chondrogenesis [16], glucose homeostasis [17], and angiogenesis [18], also reportedly possesses different modes of actions from BMP-2 with regard to new bone formation. Leblanc et al. [19] showed that BMP-9 induces heterotrophic ossification in damaged but not undamaged skeletal muscles, whereas BMP-2 caused it in both. Moreover, BMP-9 has been demonstrated to possess more osteogenic activity than BMP-2 [13, 20–22] and is resistant to noggin, a BMP antagonist [23–25]. With regard to bone formation, various studies using a recombinant BMP-9-expressing adenovirus (adBMP-9) system have shown that adBMP-9 induces robust and mature ectopic bone formation when compared to adBMP2 and may transduce osteogenic signaling differently from BMP-2, BMP-6, and BMP-7 [13, 26, 27].

In our previous studies, we demonstrated that rhBMP-9/ACS has greater osteogenic potential than surgical control and ACS alone for treatment of rat calvarial defects [28, 29]. It has further been shown that the combination of collagen membranes with rhBMP-9 significantly enhanced alkaline phosphatase mRNA expression and alizarin red staining compared with rhBMP-2 [21]. However, the difference in bone regenerative activity between rhBMP-2 and rhBMP-9 remains unknown. The calvarial critical-size defects (CSD) model (calvarial defects with a diameter of 5 mm) without spontaneous healing is considered effective for evaluating bone regenerative effects of various biomaterials and treatment modalities because of its convenience, reproducibility and relatively slight surgical invasion [28–32]. Thus, the aim of this study was to compare the effect of rhBMP-2 and rhBMP-9 with ACS on new bone formation by using a rat calvarial CSD model.

Materials and methods

Experimental animals

This study included 28 male Wistar rats, aged 17 weeks, (Kyudo Co. Ltd., Tosu, Japan) housed in a light- and temperature-controlled environment (23 ± 1 °C, 40–70% humidity, with a 12-h light/dark cycle) with free access to rodent food and water ad libitum throughout the experimental period. All animal experimental protocols and procedures (in-life phase from January 22, 2015 to February 5, 2015 or January 26, 2015 to March 26, 2015) were approved by the Ethical Committee of the Animal Research Center of Kagoshima University, Japan (D14023).

Surgical procedures

One surgeon (T. N.) performed all surgical procedures under general and local anesthesia using aseptic routines. General anesthesia was administered by intra-abdominal injection of pentobarbital sodium (40 mg/kg somnopentyl; Kyoritsu Seiyaku Co., Tokyo, Japan). Local infiltration anesthesia (xylocaine; Fujisawa Inc., Osaka, Japan) was administered at surgical sites before surgery. The surgical part of the cranium was shaved and an approximately 20-mm sagittal incision was made across the scalp of the animal. A flap was raised to expose the calvarial bone and a standardized, two circular, through-through bone defects (5 mm in diameter) separated by a distance of 2 mm or more were created in the midportion of parietal bones both sides of the midsagittal suture using a slow-speed trephine bur (Stoma; Emmingen-Liptingen, Germany) with saline irrigation to prevent heat damage to the host bone. The trephined calvarial bone disk (1–1.5 mm in depth) was removed to avoid damage to the dura. Bilateral calvarial defects (n = 56) were allocated into four groups (14 sites for each group): absorbable collagen sponge (CollaTape, Zimmer Dental, Carlsbad, CA, USA) alone (ACS), rhBMP-2 with ACS (rhBMP-2/ACS), rhBMP-9 with ACS (rhBMP-9/ACS), or underwent sham surgery as a control, on the condition that the treatments of rhBMP-2/ACS and rhBMP-9/ACS (to avoid a crossover effect between rhBMP-2 and rhBMP-9), or the same treatments were not included in the same animal. According to the previous report [33], the concentration of rhBMP-2 and rhBMP-9 was set at a reasonable dose of rhBMP-2 (2.5 μg). For ACS-treated groups, ACS was loaded with sterilized saline before being applied to the defect. rhBMP-2 (PeproTech, Rocky Hill, NJ, USA) and rhBMP-9

(Wako Pure Chemical Industries Ltd., Osaka, Japan) were reconstituted and diluted in sterilized saline. Prior to rhBMP-2/ACS or rhBMP-9/ACS implantation, ACS was saturated with rhBMP-2 or rhBMP-9 solution and allowed to rest for 30 min. After implantation, the periosteum was repositioned and closed with a 7-0 absorbable suture (Vicryl, Johnson & Johnson Pty Ltd., Tokyo, Japan) and the skin was closed with a 6-0 nylon suture (Nesco Suture, Alfresa Pharma Co., Osaka, Japan). All the animals received a subcutaneous antibiotic and analgesic: 25 mg/kg ceftriaxone (Rocephin; Chugai Pharmaceutical Co, Tokyo, Japan) and 4 mg/kg carprofen (Rimadyl; Zoetis, Tokyo, Japan), respectively, for 3 days. Animals were euthanized by overdose injection of pentobarbital sodium at 2 and 8 weeks after reconstructive surgery, and 7 samples from each group were examined at each time point.

Micro-computed tomography (μ-CT) analysis

Calvariae, including the defect areas, were dissected out and fixed in 10% neutral-buffered formalin, before being scanned with a Skyscan 1174 compact micro (μ)-CT (Bruker MicroCT, Kontich, Belgium) at 52 kV/800 μA with a Ti-0.5 filter. The entire appearance and central portion of each defect (including margin with maximum linear length) were observed to obtain optimal histological sections and quantify bone volume (BV) within defects. Scanned CT images were processed in Digital Imaging and Communications in Medicine format, and three-dimensional (3D) images were constructed using instrumentation software. For calvarial defects, a cylindrical region of interest (ROI) with a diameter of 5 mm and height comprising the total depth was chosen. BV at the ROI was measured using the CT Analyzer software (Bruker MicroCT).

Histologic and histomorphometric analyses

Formalin-fixed samples were further trimmed and decalcified in 10% formic acid solution, then dehydrated, and embedded in paraffin. Serial sections of 6 μm thickness were prepared along the coronal plane, stained with hematoxylin and eosin (H&E), and then examined under a light microscope (BX51, Olympus Corp., Tokyo, Japan). Images of the three most central serial sections of defects were acquired and histomorphometric measurements were performed by a single experienced and masked examiner (Y. S.) using image-analysis software (WinROOF2015, Mitani Co., Tokyo, Japan) and to use mean values obtained from the three evaluations. The following parameters were measured: (1) distance between the margins of the original surgical defect (defect length: DL); (2) length of the internal bone bridging formation (defect closure: DC); (3) total defect area (TA), as determined by first identifying the external and internal surfaces of the original calvarium at the right and left margins of the surgical defect, and then connecting them with lines drawn along their respective curvatures; (4) H&E-stained region in the TA, which was color-extracted and defined as newly formed bone area (NBA), bone marrow area (BMA), and adipose tissue area (ATA) in the NBA; and (5) vertical augmentation height as measured at four points, two 1-mm apart in the center of the defect and two 1-mm interior from defect margins, with each pair of measurements averaged to yield mean central bone height (CBH) and marginal bone height (MBH). These heights were composed of calcified osseous tissue, grafted ACS, and/or the soft tissue interface [34]. The TA, NBA, BMA, and ATA were measured in square millimeters, while NBA was calculated as percentage of TA, and BMA and ATA were calculated as percentages of NBA. Linear measurement of DC was calculated as percentage of defect length within each defect. Each measured values of each group (DL, DC, TA, NBA, BMA, and ATA) are shown in Table 1.

Statistical analyses

A nonparametrical analysis of variance (Kruskal-Wallis test) was used to detect statistically significant differences between the treatments of the different groups. When the Kruskal-Wallis test was significant, Steel-Dwass post hoc test was performed for multiple comparisons. Results were considered statistically significant at $P < 0.05$. Statistical analyses were performed using statistical software (BellCurve for Excel, Social Survey Research Information Co., Ltd., Tokyo, Japan). All results are expressed as means ± SD.

Table 1 Histomorphometric data of linear and area measurements in each treatment group at 2 and 8 weeks post-surgery (means ± SD)

Histomorphometric parameter	Experimental condition			
	Control	ACS	rhBMP-2/ACS	rhBMP-9/ACS
	2 weeks			
	$N = 7$	$N = 7$	$N = 7$	$N = 7$
DL (mm)	4.95 ± 0.06	4.99 ± 0.03	4.93 ± 0.03	4.91 ± 0.10
DC (mm)	2.09 ± 0.30	2.13 ± 0.97	4.23 ± 1.34	2.89 ± 1.03
TA (mm^2)	4.76 ± 0.21	4.97 ± 0.25	5.01 ± 0.28	1.18 ± 0.44
NBA (mm^2)	0.90 ± 0.12	0.96 ± 0.43	2.34 ± 1.00	1.18 ± 0.44
	8 weeks			
	$N = 7$	$N = 7$	$N = 7$	$N = 7$
DL (mm)	4.99 ± 0.04	4.94 ± 0.06	4.93 ± 0.11	4.96 ± 0.05
DC (mm)	2.75 ± 1.14	3.84 ± 0.86	4.89 ± 0.15	4.95 ± 0.06
TA (mm^2)	4.83 ± 0.13	4.84 ± 0.14	4.96 ± 0.11	4.84 ± 0.12
NBA (mm^2)	1.67 ± 0.64	2.27 ± 0.92	3.44 ± 0.57	3.31 ± 0.55
BMA (mm^2)	0.01 ± 0.01	0.07 ± 0.06	0.51 ± 0.17	0.23 ± 0.19
ATA (mm^2)	0.00 ± 0.01	0.02 ± 0.03	0.31 ± 0.12	0.12 ± 0.12

Results

In vivo findings

Postoperative clinical healing was uneventful in all 56 sites, except limited signs of inflammation until a few days post-surgery. No visible complications, such as material exposure, infection, or suppuration, were observed during the rest of the experimental period.

μ-CT analysis

Representative 3D μ-CT images are shown in Fig. 1. After 2 weeks of healing, broad radiolucent areas and some marginal bone formation occurred from the margin of defects in control, ACS, and rhBMP-9/ACS groups, while an increase in the radiopacity within the defects was observed in the rhBMP-2/ACS group. In addition, an increased radiopacity of the entire defect was observed in three samples for the rhBMP-2/ACS group. After 8 weeks of healing, non-uniform and minimal bone formation from the margin of defects was observed in control and ACS groups. In contrast, defects treated with rhBMP-2/ACS or rhBMP-9/ACS displayed more increased radiopacity of the entire defect compared with that in 2 weeks of healing periods. All samples in rhBMP-2/ACS group (n = 7) and rhBMP-9/ACS group (n = 7) were observed to be filled with radiopacles for the most part within bone defects at 8 weeks. BV within bone defects are shown in Fig. 2. After 2 weeks of healing (Fig. 2a), BV was higher in the rhBMP-2/ACS group (5.44 ± 3.65 mm^3, n = 7) compared to the other groups (control 1.60 ± 1.14 mm^3, ACS 1.42 ± 0.60 mm^3, and rhBMP-9/ACS 1.68 ± 0.51 mm^3, n = 7, respectively). After 8 weeks (Fig. 2b), BV in rhBMP-2/ACS and rhBMP-9/ACS groups (18.17 ± 2.51 and 16.30 ± 2.46 mm^3, n = 7, respectively) was significantly higher than that in the control and ACS groups (6.02 ± 2.90 and 9.30 ± 2.75 mm^3, n = 7, respectively), and no significant difference was detected between rhBMP-2/ACS and rhBMP-9/ACS groups.

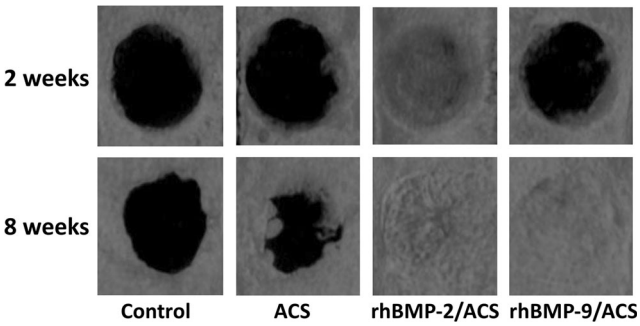

Fig. 1 Three dimensionally reconstructed radiographic images of representative rat calvarial defects after 2 and 8 weeks of healing

Descriptive histology

The control group demonstrated limited or minimal new bone formation at 2 and 8 weeks (Figs. 3a and 4a). Most of the defects were occupied by connective tissue composed of large numbers of collagen fibers parallel to the wound defect (Figs. 3b and 4b). Furthermore, volumetric shrinkage of defects was predominantly observed in the control group.

At 2 weeks, sites receiving ACS alone showed somewhat greater osteogenic bone formation compared with sites receiving sham surgery (Fig. 3c). However, most defects were considerably occupied by provisional connective tissue and ACS fragments (Fig. 3d). New bone formation was generally limited to defect margins in the ACS group (Fig. 3c). After 8 weeks, implanted ACS was completely adsorbed and new bone formation, progressing from the edge of defects toward their center, was enhanced compared with observations of this group at 2 weeks (Fig. 4c, d).

In the rhBMP-2/ACS group, new bone formation in the defect was enhanced at 2 weeks (Fig. 3e). Furthermore, newly formed bone had intensively penetrated into the ACS material, with remnants of ACS enveloped in newly formed woven bone (Fig. 3f). At 8 weeks, newly formed bone expanded and developed into highly mineralized trabecular bone with abundant lacuna consisting of many osteocytes, vessels, and bone marrow (Fig. 4e, f). Despite this, large fatty marrow spaces were also dominant in newly formed bone in the rhBMP-2/ACS group (Fig. 4f).

At 2 weeks, the rhBMP-9/ACS group showed a limited increase in bone formation, primarily at the edge of defects (Fig. 3g). No remarkable difference could be noted between ACS and rhBMP-9/ACS groups. In the rhBMP-9/ACS group, most of the defects were filled with residual ACS fragments and non-mineralized connective tissue, which was accompanied by a delicate network of trabeculae formed by woven bone (Fig. 3g, h). At 8 weeks, the rhBMP-9/ACS group showed robust re-establishment of bone formation including trabecular bone with cell-rich fibrovascular tissue (Fig. 4g). Compared to the rhBMP-2/ACS group, newly formed bone was denser, had less fatty marrow, and contained many more osteocytes in the rhBMP-9/ACS group (Fig. 4h). Furthermore, new bone in this group exhibited a morphology that was more similar to native host bone at 8 weeks compared with the rhBMP-2/ACS group.

Histomorphometric analysis

Results from the histomorphometric analyses after 2- and 8-week healing periods are shown in Figs. 5 and 6, respectively. An average percentage of DC by newly formed bone (DC/DL) in the rhBMP-2/ACS group (85.88 ± 27.29%, n = 7) was greater than that in other groups (control 42.30 ± 6.22%, ACS 42.67 ± 19.51%, and rhBMP-9/ACS 58.99 ± 21.64%, n = 7,

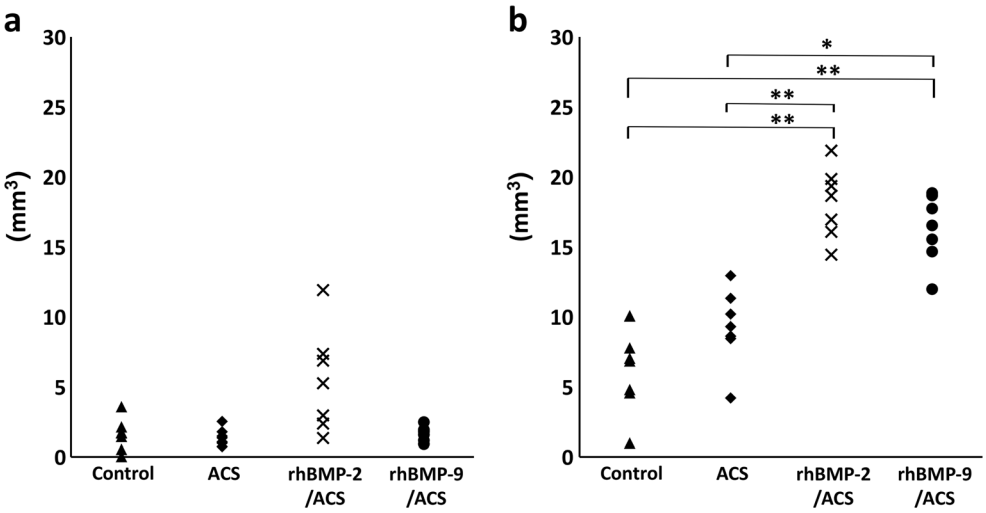

Fig. 2 Data distribution of bone volume for each treatment group in rat calvarial defects at 2 (**a**) and 8 weeks (**b**). *$P < 0.05$, **$P < 0.01$

respectively) at 2 weeks (Fig. 5a). NBA/TA in the rhBMP-2/ACS group (46.61 ± 20.12%, $n = 7$) was higher than that in the other groups (control 18.99 ± 3.02%, ACS 19.17 ± 8.10%, and rhBMP-9/ACS 24.73 ± 9.69%, $n = 7$, respectively) at 2 weeks (Fig. 5d). After 8 weeks, DC/DL and CBH in rhBMP-2/ACS and rhBMP-9/ACS groups (DC/DL 99.04 ± 2.55 and 99.85 ± 0.39%, CBH 0.93 ± 0.14 and 0.86 ± 0.09 mm, $n = 7$, respectively) were significantly higher than those in the control and ACS groups (DC/DL 55.15 ± 23.20 and 77.74 ± 17.27%, CBH 0.41 ± 0.11 and 0.56 ± 0.25 mm, $n = 7$, respectively) (Fig. 6a, b). Further, NBA/TA in rhBMP-2/ACS and rhBMP-9/ACS groups (69.41 ± 11.71 and 68.36 ± 9.98%, $n = 7$, respectively) was significantly greater than that in the control group (34.50 ± 13.27%, $n = 7$) (Fig. 6d). Finally, BMA/NBA and ATA/NBA in rhBMP-2/ACS and rhBMP-9/ACS groups (BMA/NBA 14.90 ± 5.19 and 6.93 ± 5.60%, $n = 7$, respectively, ATA/NBA 9.24 ± 3.72 and 3.37 ± 3.17%, $n = 7$, respectively) were significantly higher than those in the control group (BMA/NBA 0.96 ± 1.01% and ATA/NBA 0.13 ± 0.35%, $n = 7$, respectively), and those in rhBMP-2/ACS were the highest among the groups at 8 weeks post-surgery (Fig. 6e, f).

Discussion

A growing number of recent reports have indicated that clinical use of rhBMP-2 for bone regeneration may cause adverse events such as tissue inflammation/swelling [35, 36] and bone resorption [37] in humans. Therefore, there is a rising need for the development of a more predictable, effective, and safe bone regenerative therapies with minimal to no complications. Recently, the use of rhBMP-9 has gained attention as a

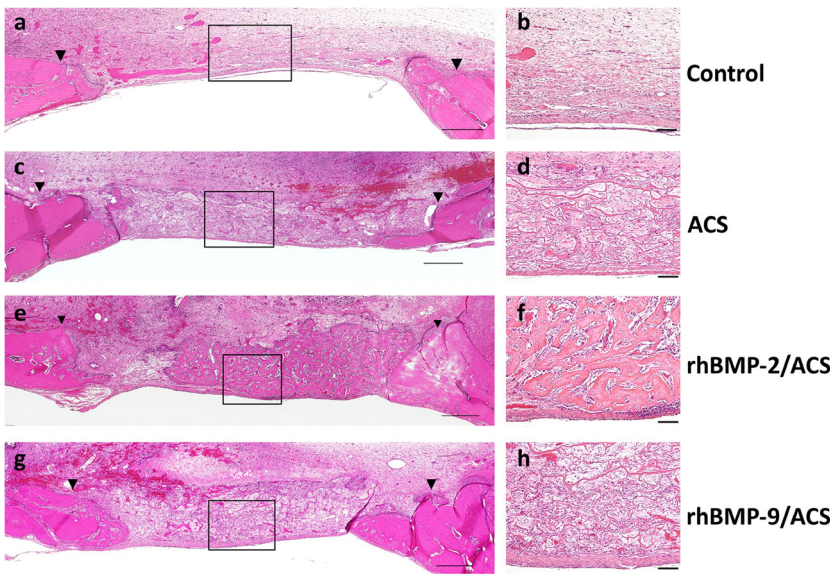

Fig. 3 Representative histologic photomicrographs of rat calvarial defects at 2 weeks post-surgery. Left panels are overviews of the defect sites treated with control (**a**), ACS (**c**), rhBMP-2/ACS (**e**), and rhBMP-9/ACS (**f**) (*scale bar*, 500 μm; H&E). *Right panels* are higher magnifications of the *inset boxes* in the each *left panels* (**b**, **d**, **f**, and **h**; *scale bar*, 100 μm; H&E). *Arrowheads* show defect margin

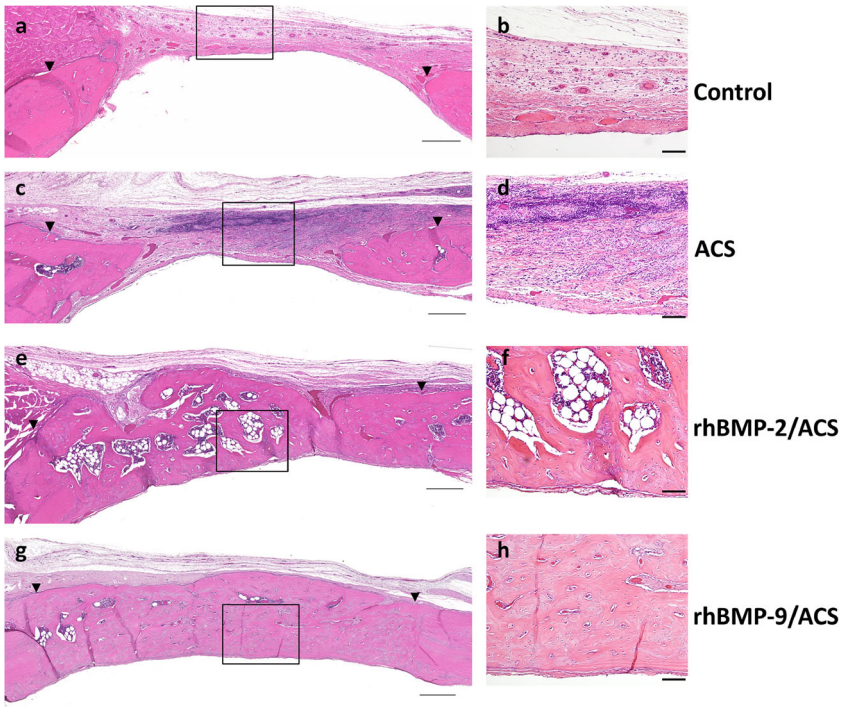

Fig. 4 Representative histologic photomicrographs of rat calvarial defects at 8 weeks post-surgery. *Left panels* are overviews of the defect sites treated with control (**a**), ACS (**c**), rhBMP-2/ACS (**e**), and rhBMP-9/ACS (**f**) (scale bar, 500 μm; H&E). *Right panels* are higher magnifications of the *inset boxes* in the each *left panels* (**b**, **d**, **f**, and **h**; *scale bar*, 100 μm; H&E). *Arrowheads* show defect margin

promising growth factor for bone regeneration, as rhBMP-9 possesses different properties than rhBMP-2 [19, 23–25] and may be utilized effectively at lower doses compared with other BMPs.

To the best of our knowledge, this is the first report comparing the effects of rhBMP-9/ACS and rhBMP-2/ACS on bone formation in rat CSD. In this study, we chose ACS as a carrier for rhBMPs, since ACS is biocompatible, biodegradable, and capable of retaining and then releasing growth factors at treatment sites of bone defects [38]. Furthermore, ACS has been extensively utilized in rat CSD; thus, our results could be corroborated with other previous investigations [29,

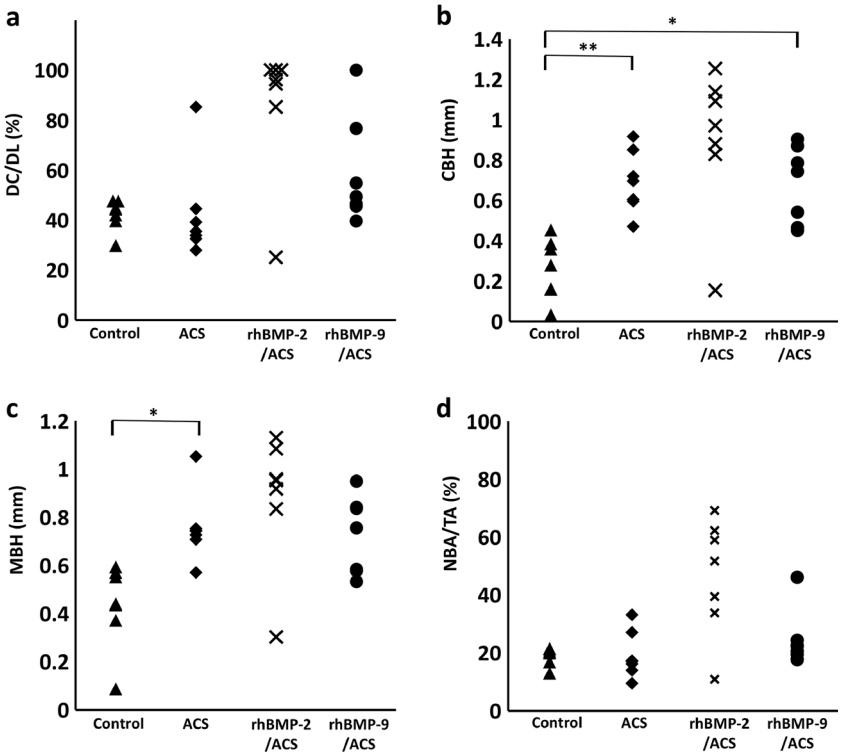

Fig. 5 Histomorphometric data of DC/DL (**a**), CBH (**b**), MBH (**c**), and NBA/TA (**d**) for each treatment group in rat calvarial defects at 2 weeks. *DC* defect closure, *DL* defect length, *CBH* central bone height, *MBH* marginal bone height, *NBA* newly formed bone area, *TA* total defect area. $^{*}P < 0.05$, $^{**}P < 0.01$

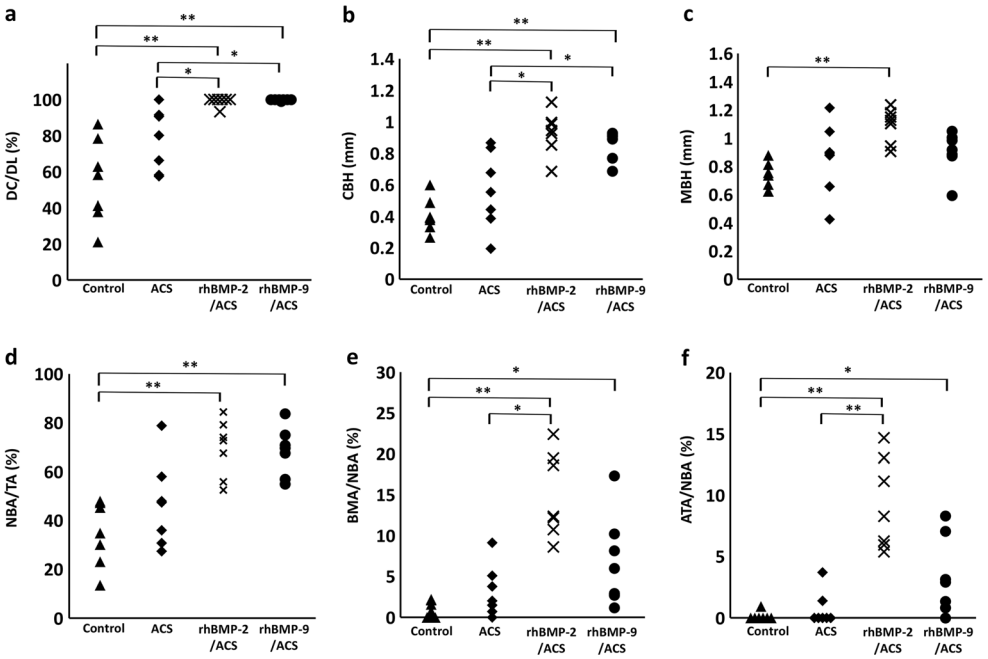

Fig. 6 Histomorphometric data of DC/DL (**a**), CBH (**b**), MBH (**c**), NBA/TA (**d**), BMA/NBA (**e**), and ATA/NBA (**f**) for each treatment group in rat calvarial defects at 8 weeks. *DC* defect closure, *DL* defect length, *CBH* central bone height, *MBH* marginal bone height, *NBA* newly formed bone area, *BMA* bone marrow area, *ATA* adipose tissue area, *TA* total defect area. $^{*}P < 0.05$, $^{**}P < 0.01$

33, 39]. Pelaez et al. [33] have demonstrated that the osteoinductive threshold of rhBMP-2/ACS in rat CSD was reached at 1.25–2.5 μg/site, with no further enhancement observed above a 2.5-μg dose. Moreover, a comparative study of BMP-2, BMP-4 and BMP-7/ACS (amount of each BMP = 2.5 μg/site) application in rat calvarial defects showed that all three BMPs induced bone formation, with no specific differences in bone regeneration potential were observed [39]. Thus, we evaluated a dosage of 2.5 μg/site for application of rhBMP-2 and rhBMP-9 in this study. However, the osteoinductive threshold of rhBMP-9 and the delivery mechanisms of ACS such as the binding and releasing kinetics of rhBMPs are still unclear. Further studies are needed to clarify these issues.

Although the rhBMP-2/ACS group demonstrated greater bone formation than other groups at an early time point of 2 weeks post-surgery, there was no statistically significant difference in quantities of newly formed bone induced by rhBMP-2/ACS and rhBMP-9/ACS at 8 weeks after surgery in this study. Furthermore, the area of adipose tissues within newly formed bone in the rhBMP-2 group was greater than that in the rhBMP-9 group at 8 weeks post-surgery. In contrast, the rhBMP-9/ACS-induced bone was more similar to the native host bone. These findings suggest that rhBMP-9 has comparable osteoinductive activity to rhBMP-2 after a healing period of 8 weeks and that the processes by which new bone formation is induced may differ between rhBMP-2 and rhBMP-9. The rhBMP-2/ACS-generated bone, which contained fatty marrow, may be explained on a molecular level by the fact that BMP-2 can also induce adipogenic differentiation through activation of the transcription factor peroxisome proliferator-activated receptor gamma, a key regulator of adipocyte commitment [40, 41]. Further in vivo studies are needed to clarify whether the adipose tissues within newly formed bone affect clinical outcomes in the bone regenerative therapy.

Our previous in vitro studies have demonstrated that rhBMP-9 potently induces osteoblastic differentiation of periodontal ligament fibroblasts and dedifferentiated fat cells compared with rhBMP-2 [20, 24]. Moreover, combination of rhBMP-9 with collagen membranes or bone-grafting materials yields more potent osteopromotive potential compared to rhBMP-2 [21, 22]. However, results from the present in vivo study suggest new bone formation was induced more slowly in the rhBMP-9/ACS group compared to the rhBMP-2/ACS group. This inconsistency between our in vitro and in vivo studies might partially be explained by the environment of wound healing existing in bone defects. During bone healing, an inflammatory cascade initiates the regeneration process. Numerous cytokines and growth factors, including BMPs and BMP antagonists, play a role in different phases of bone healing [42–44]. It has been demonstrated that FGF-2, an important factor for bone healing/regeneration, is secreted from macrophages at bone fracture sites during initial stages [44]. Synergistic effects of FGF-2 on BMP-2-induced osteogenesis have also been reported [45]. In contrast, the combination of BMP-9 and FGF-2 synergistically induced proliferation of mesenchymal stem cells, although FGF-2 inhibited BMP-9-induced osteogenic differentiation of these cells [46]. These studies likely indicate that synergistic effects between FGF-2 and BMP-2 or BMP-9 are regulated by different modes of action. In addition, activin A, which plays a crucial role in tissue repair, fibrosis, and inflammation [47], has been reported to antagonize BMP-9, but not BMP-2 [48]. Thus,

differences in osteogenic activity between rhBMP-2 and rhBMP-9 observed in this study may result from different actions of several factors expressed during the healing process in vivo. Furthermore, Sreekumar et al. recently investigated the effect of rhBMP7 and rhBMP9 on primary human osteoblasts from 110 donors and compared them to rhBMP2. It was found that rhBMP9 induced the highest levels of osteoblast activity when compared to the clinically utilized rhBMP2 and rhBMP7 and suggested rhBMP9 as a possible alternative strategy for bone tissue regenerative strategies [49]. Therefore, further studies to better characterize cellular pathways involved during BMP-9-induced osteogenesis are necessary.

Within the limits of this study, it can be concluded that rhBMP-2/ACS led to a faster new bone formation at 2 weeks and that rhBMP-9/ACS provided new bone formation with less adipose tissues compared with rhBMP-2/ACS in rat CSD at 8 weeks post-surgery. However, the results obtained from the CSD model may not be applicable to alveolar bone since the anatomy is different and the surgical area is isolated from oral environment [50]. Further research investigating the potential of rhBMP-9/ACS as a therapeutic system for future oral and periodontal reconstructive procedures and medical fields is still necessary, and mechanisms underlying the effects of rhBMP-9 on bone regeneration must be elucidated prior to clinical use in humans.

Acknowledgements The authors are grateful to Dr. Chihaya Koriyama, Department of Epidemiology and Preventive Medicine at Kagoshima University Graduate School of Medical and Dental Sciences, Kagoshima, Japan, for her assistance in performing the statistical analysis.

Compliance with ethical standards

Conflict of interest The authors declare that they have no conflicts of interests.

Funding This study was supported by Grants-in-Aid for Scientific Research (B) (No.24792147) and (C) (No.26462972) from the Japan Society for the Promotion of Science (JSPS).

Ethical approval All animal experimental protocols and procedures were approved by the Ethical Committee of the Animal Research Center of Kagoshima University, Japan (D14023).

Informed consent Informed consent was not required in this study.

References

1. Schliephake H (2002) Bone growth factors in maxillofacial skeletal reconstruction. Int J Oral Maxillofac Surg 31:469–484
2. Taba M, Jin Q, Sugai JV, Giannobile WV (2005) Current concepts in periodontal bioengineering. Orthod Craniofac Res 8:292–302
3. Herford AS, Boyne PJ (2008) Reconstruction of mandibular continuity defects with bone morphogenetic protein-2 (rhBMP-2). J Oral Maxillofac Surg 66:616–624
4. Jovanovic SA, Hunt DR, Bernard GW, Spiekermann H, Wozney JM, Wikesjo UM (2007) Bone reconstruction following implantation of rhBMP-2 and guided bone regeneration in canine alveolar ridge defects. Clin Oral Implants Res 18:224–230
5. Kinsella CR Jr, Bykowski MR, Lin AY, Cray JJ, Durham EL, Smith DM, DeCesare GE, Mooney MP, Cooper GM, Losee JE (2011) BMP-2-mediated regeneration of large-scale cranial defects in the canine: an examination of different carriers. Plast Reconstr Surg 127:1865–1873
6. Selvig KA, Sorensen RG, Wozney JM, Wikesjo UM (2002) Bone repair following recombinant human bone morphogenetic protein-2 stimulated periodontal regeneration. J Periodontol 73:1020–1029
7. Dickinson BP, Ashley RK, Wasson KL, O'Hara C, Gabbay J, Heller JB, Bradley JP (2008) Reduced morbidity and improved healing with bone morphogenic protein-2 in older patients with alveolar cleft defects. Plast Reconstr Surg 121:209–217
8. Walker DH, Wright NM (2002) Bone morphogenetic proteins and spinal fusion. Neurosurg Focus 13:e3
9. Neovius E, Lemberger M, Docherty Skogh AC, Hilborn J, Engstrand T (2013) Alveolar bone healing accompanied by severe swelling in cleft children treated with bone morphogenetic protein-2 delivered by hydrogel. J Plast Reconstr Aesthet Surg 66:37–42
10. Woo EJ (2012) Adverse events reported after the use of recombinant human bone morphogenetic protein 2. J Oral Maxillofac Surg 70:765–767
11. Zara JN, Siu RK, Zhang X, Shen J, Ngo R, Lee M, Li W, Chiang M, Chung J, Kwak J, Wu BM, Ting K, Soo C (2011) High doses of bone morphogenetic protein 2 induce structurally abnormal bone and inflammation in vivo. Tissue Eng Part A 17:1389–1399
12. Cheng H, Jiang W, Phillips FM, Haydon RC, Peng Y, Zhou L, Luu HH, An N, Breyer B, Vanichakarn P, Szatkowski JP, Park JY, He TC (2003) Osteogenic activity of the fourteen types of human bone morphogenetic proteins (BMPs). J Bone Joint Surg Am 85-A: 1544–1552
13. Kang Q, Sun MH, Cheng H, Peng Y, Montag AG, Deyrup AT, Jiang W, Luu HH, Luo J, Szatkowski JP, Vanichakarn P, Park JY, Li Y, Haydon RC, He TC (2004) Characterization of the distinct orthotopic bone-forming activity of 14 B.P. using recombinant adenovirus-mediated gene delivery. Gene Ther 11:1312–1320
14. Lopez-Coviella I, Berse B, Krauss R, Thies RS, Blusztajn JK (2000) Induction and maintenance of the neuronal cholinergic phenotype in the central nervous system by BMP-9. Science 289:313–316
15. Lord E, Bergeron E, Senta H, Park H, Faucheux N (2010) Effect of BMP-9 and its derived peptide on the differentiation of human white preadipocytes. Growth Factors 28:149–156
16. Majumdar MK, Wang E, Morris EA (2001) BMP-2 and BMP-9 promotes chondrogenic differentiation of human multipotential mesenchymal cells and overcomes the inhibitory effect of IL-1. J Cell Physiol 189:275–284
17. Chen C, Grzegorzewski KJ, Barash S, Zhao Q, Schneider H, Wang Q, Singh M, Pukac L, Bell AC, Duan R, Coleman T, Duttaroy A, Cheng S, Hirsch J, Zhang L, Lazard Y, Fischer C, Barber MC, Ma ZD, Zhang YQ, Reavey P, Zhong L, Teng B, Sanyal I, Ruben SM, Blondel O, Birse CE (2003) An integrated functional genomics screening program reveals a role for BMP-9 in glucose homeostasis. Nat Biotechnol 21:294–301
18. Ricard N, Ciais D, Levet S, Subileau M, Mallet C, Zimmers TA, Lee SJ, Bidart M, Feige JJ, Bailly S (2012) BMP9 and BMP10 are critical for postnatal retinal vascular remodeling. Blood 119:6162–6171
19. Leblanc E, Trensz F, Haroun S, Drouin G, Bergeron E, Penton CM, Montanaro F, Roux S, Faucheux N, Grenier G (2011) BMP-9-

induced muscle heterotopic ossification requires changes to the skeletal muscle microenvironment. J Bone Miner Res 26:1166–1177
20. Fuchigami S, Nakamura T, Furue K, Sena K, Shinohara Y, Noguchi K (2016) Recombinant human bone morphogenetic protein-9 potently induces osteogenic differentiation of human periodontal ligament fibroblasts. Eur J Oral Sci 124:151–157
21. Fujioka-Kobayashi M, Sawada K, Kobayashi E, Schaller B, Zhang Y, Miron RJ (2016) Recombinant human bone morphogenetic protein 9 (rhBMP9) induced osteoblastic behaviour on a collagen membrane compared with rhBMP2. J Periodontol 87:e101–e107
22. Fujioka-Kobayashi M, Sawada K, Kobayashi E, Schaller B, Zhang Y, Miron RJ (2016) Osteogenic potential of rhBMP9 combined with a bovine-derived natural bone mineral scaffold compared to rhBMP2. Clin Oral Implants Res. doi:10.1111/clr.12804
23. Rosen V (2006) BMP and BMP inhibitors in bone. Ann N Y Acad Sci 1068:19–25
24. Nakamura T, Shinohara Y, Momozaki S, Yoshimoto T, Noguchi K (2013) Co-stimulation with bone morphogenetic protein-9 and FK506 induces remarkable osteoblastic differentiation in rat dedifferentiated fat cells. Biochem Biophys Res Commun 440:289–294
25. Wang Y, Hong S, Li M, Zhang J, Bi Y, He Y, Liu X, Nan G, Su Y, Zhu G, Li R, Zhang W, Wang J, Zhang H, Kong Y, Shui W, Wu N, He Y, Chen X, Luu HH, Haydon RC, Shi LL, He TC, Qin J (2013) Noggin resistance contributes to the potent osteogenic capability of BMP9 in mesenchymal stem cells. J Orthop Res 31:1796–1803
26. Li JZ, Li H, Sasaki T, Holman D, Beres B, Dumont RJ, Pittman DD, Hankins GR, Helm GA (2003) Osteogenic potential of five different recombinant human bone morphogenetic protein adenoviral vectors in the rat. Gene Ther 10:1735–1743
27. Luu HH, Song WX, Luo X, Manning D, Luo J, Deng ZL, Sharff KA, Montag AG, Haydon RC, He TC (2007) Distinct roles of bone morphogenetic proteins in osteogenic differentiation of mesenchymal stem cells. J Orthop Res 25:665–677
28. Shinohara Y, Nakamura T, Shirakata Y, Noguchi K (2016) Bone healing capabilities of recombinant human bone morphogenetic protein-9 (rhBMP-9) with a chitosan or collagen carrier in rat calvarial defects. Dent Mater J 35:454–460
29. Nakamura T, Shirakata Y, Shinohara Y, Miron RJ, Furue K, Noguchi K (2016) Osteogenic potential of recombinant human bone morphogenetic protein-9/absorbable collagen sponge (rhBMP-9/ACS) in rat critical size calvarial defects. Clin Oral Investig. doi:10.1007/s00784-016-1963-4
30. Vajgel A, Mardas N, Farias BC, Petrie A, Cimoes R, Donos N (2014) A systematic review on the critical size defect model. Clin Oral Implants Res 25:879–893
31. Donos N, Lang NP, Karoussis IK, Bosshardt D, Tonetti M, Kostopoulos L (2004) Effect of GBR in combination with deproteinized bovine bone mineral and/or enamel matrix proteins on the healing of critical-size defects. Clin Oral Implants Res 15:101–111
32. Luvizuto ER, Tangl S, Zanoni G, Okamoto T, Sonoda CK, Gruber R, Okamoto R (2011) The effect of BMP-2 on the osteoconductive properties of beta-tricalcium phosphate in rat calvaria defects. Biomaterials 32:3855–3861
33. Pelaez M, Susin C, Lee J, Fiorini T, Bisch FC, Dixon DR, McPherson JC 3rd, Buxton AN, Wikesjo UM (2014) Effect of rhBMP-2 dose on bone formation/maturation in a rat critical-size calvarial defect model. J Clin Periodontol 41:827–836
34. Artzi Z, Kozlovsky A, Nemcovsky CE, Moses O, Tal H, Rohrer MD, Prasad HS, Weinreb M (2008) Histomorphometric evaluation of natural mineral combined with a synthetic cell-binding peptide (P-15) in critical-size defects in the rat calvaria. Int J Oral Maxillofac Implants 23:1063–1070
35. Tumialan LM, Rodts GE (2007) Adverse swelling associated with use of rh-BMP-2 in anterior cervical discectomy and fusion. Spine J 7:509–510
36. Smucker JD, Rhee JM, Singh K, Yoon ST, Heller JG (2006) Increased swelling complications associated with off-label usage of rhBMP-2 in the anterior cervical spine. Spine 31:2813–2819
37. McClellan JW, Mulconrey DS, Forbes RJ, Fullmer N (2006) Vertebral bone resorption after transforaminal lumbar interbody fusion with bone morphogenetic protein (rhBMP-2). J Spinal Disord Tech 19:483–486
38. Seeherman H, Wozney JM (2005) Delivery of bone morphogenetic proteins for orthopedic tissue regeneration. Cytokine Growth Factor Rev 16:329–345
39. Hyun SJ, Han DK, Choi SH, Chai JK, Cho KS, Kim CK, Kim CS (2005) Effect of recombinant human bone morphogenetic protein-2, -4, and -7 on bone formation in rat calvarial defects. J Periodontol 76:1667–1674
40. Takada I, Kouzmenko AP, Kato S (2009) Wnt and PPARgamma signaling in osteoblastogenesis and adipogenesis. Nat Rev Rheumatol 5:442–447
41. Rosen ED, Spiegelman BM (2001) PPARgamma: a nuclear regulator of metabolism, differentiation, and cell growth. J Biol Chem 276:37731–37734
42. Minkwitz S, Fassbender M, Kronbach Z, Wildemann B (2015) Longitudinal analysis of osteogenic and angiogenic signaling factors in healing models mimicking atrophic and hypertrophic nonunions in rats. PLoS One 10:e0124217
43. Marsell R, Einhorn TA (2009) The role of endogenous bone morphogenetic proteins in normal skeletal repair. Injury 40(Suppl 3):S4–S7
44. Bolander ME (1992) Regulation of fracture repair by growth factors. Proc Soc Exp Biol Med 200:165–170
45. Kaewsrichan J, Wongwitwichot P, Chandarajoti K, Chua KH, Ruszymah BH (2011) Sequential induction of marrow stromal cells by FGF2 and BMP2 improves their growth and differentiation potential in vivo. Arch Oral Biol 56:90–101
46. Song T, Wang W, Xu J, Zhao D, Dong Q, Li L, Yang X, Duan X, Liang Y, Xiao Y, Wang J, He J, Tang M, Wang J, Luo J (2013) Fibroblast growth factor 2 inhibits bone morphogenetic protein 9-induced osteogenic differentiation of mesenchymal stem cells by repressing Smads signaling and subsequently reducing Smads dependent up-regulation of ALK1 and ALK2. Int J Biochem Cell Biol 45:1639–1646
47. Werner S, Alzheimer C (2006) Roles of activin in tissue repair, fibrosis, and inflammatory disease. Cytokine Growth Factor Rev 17:157–171
48. Olsen OE, Wader KF, Hella H, Mylin AK, Turesson I, Nesthus I, Waage A, Sundan A, Holien T (2015) Activin A inhibits BMP-signaling by binding ACVR2A and ACVR2B. Cell Commun Signal 13:27
49. Sreekumar V, Aspera-Werz RH, Tendulkar G, Reumann MK, Freude T, Breitkopf-Heinlein K, Dooley S, Pscherer S, Ochs BG, Flesch I, Hofmann V, Nussler AK, Ehnert S (2016) BMP9 a possible alternative drug for the recently withdrawn BMP7? New perspectives for (re-)implementation by personalized medicine. Arch Toxicol. doi:10.1007/s00204-016-1796-6
50. Pellegrini G, Seol YJ, Gruber R, Giannobile WV (2009) Preclinical models for oral and periodontal reconstructive therapies. J Dent Res 88:1065–1076